

Original Article

VEGF-C-VEGFR3/Flt4 axis regulates mammary tumor growth and metastasis in an autocrine manner

Michelle L Varney, Rakesh K Singh

Department of Pathology and Microbiology, The University of Nebraska Medical Center, 985900 Nebraska Medical Center, Omaha, NE 68198-5900

Received November 26, 2014; Accepted January 5, 2015; Epub January 15, 2015; Published February 1, 2015

Abstract: *Purpose:* Lymphangiogenic factors, such as vascular endothelial growth factor-C (VEGF-C) and VEGFC-D, and their receptor, VEGF receptor-3 (VEGFR3), play a pivotal role in the promotion of metastasis to regional lymph nodes. In the present study we explored the role of VEGF-C as an autocrine growth factor for breast cancer cells. *Methods:* We examined the expression of VEGF-C and VEGFR3 in mammary tumor cells lines and examined whether blocking the VEGF-C-VEGFR3/Flt4 pathway using a VEGFR3 antagonist would inhibit proliferation of mammary tumor cells resulting in a decrease in tumor growth and metastasis. *Results:* We report expression of VEGF-C and its receptor VEGFR3 by mammary tumor cells, and their association with aggressiveness. Inhibition of VEGF-C-VEGFR3/Flt4 in mammary tumor cells decreased their proliferation and survival. Mammary tumor bearing mice treated with a VEGFR3 antagonist showed a significant decrease in tumor growth and the extent of spontaneous and experimental lung metastases. *Conclusion:* These findings demonstrate the VEGF-C-VEGFR3/Flt4 autocrine signaling pathway regulates mammary tumor cell survival and proliferation and that neutralization of VEGFR3 signaling might lead to development of a novel therapeutic approach for malignant breast cancer.

Keywords: Breast cancer, vascular endothelial growth factor-C, vascular endothelial growth factor receptor-3, lymphangiogenesis, metastasis

Introduction

Breast cancer is the most common female cancer affecting 1 in 8 women in the United States in their lifetime [1]. After lung cancer, it is the second leading cause of cancer death in women [1]. It is estimated that in 2014 over 232,000 women will be diagnosed with the disease and that more than 40,000 will die from the disease. While detection and treatment can improve survival it is estimated that up to 6-10% of women who present with disease already have metastases [2]. Many studies have shown the most common sites for breast cancer metastases are the lymph nodes, bone, lung, liver and brain [2]. The presence of lymph node metastases in particular, has been implicated as a poor prognostic factor in breast cancer [3].

Vascular endothelial growth factor (VEGF)-C is a member of the platelet-derived growth factor family. It binds to VEGFR-3, one in a family of

receptor tyrosine kinases that play key roles in angiogenesis and lymphangiogenesis. However, there is emerging evidence supporting the role of the VEGF-C/VEGFR3 axis in promoting tumor growth and metastasis [4]. Specifically, VEGFR3 expression was found to be higher in human breast cancer specimens as compared to normal tissue [5]. The authors suggest a role for VEGFR3 as an early event in breast cancer progression that may function as a survival signal. Inhibition of VEGFR3 using antibody targeting showed that interference with VEGFR3 ligand binding inhibited primary tumor growth in a number of primary tumors [6]. We have previously shown that inhibition of VEGF-C using shRNA decreased tumor growth and metastasis of mammary tumor cells [7]. In addition, MAZ51, a cell permeable receptor tyrosine kinase inhibitor has been shown to block the proliferation of human endothelial cells as well as inhibit the growth of rat mammary carcinomas [8]. With these observations we hypothesized that the VEGF-C-VEGFR3/Flt4-dependent

VEGFR3/Flt4 autocrine pathway in mammary tumor cells

autocrine signaling pathway plays an important role in breast cancer growth, progression and metastasis.

Materials and methods

Cell lines and reagents

Three murine mammary adenocarcinoma cell lines differing in their metastatic potential, 4T1 (highly metastatic), Cl66 (moderately metastatic) and Cl66M2 (poorly metastatic) were used in this study. Cells were maintained in Dulbecco's Modified Eagle Media (DMEM) (Mediatech, Henderson, VA) with 5% serum supreme (Biowhitaker, Walkersville, MD), 1% vitamins, 1% L-glutamine and 0.08% gentamycin (Invitrogen, Carlsbad, CA). MAZ51, a VEGFR3 specific inhibitor was purchased from EMD Biosciences (San Diego, CA).

mRNA analysis

Total cellular RNA was isolated using Trizol® (Invitrogen) reagent according to the manufacturer's protocol. 5 µg of total RNA was subjected to Superscript-II-(Invitrogen) mediated reverse transcription. cDNA was analyzed by semi-quantitative reverse transcriptase-based PCR. The following primers, VEGFR3 5'-GCTGTGGTTGGAGAGAAG-3' and 5'-GGTCAGGATGCTGGAGAG-3', VEGF-C 5'-CTACAGATGTGGGGT-TGCT-3' and 5'-GCTGCCTGACACTGTGGTAA-3' and GAPDH 5'-AGCCTCGTCCCGTAGACAAAA-3' and 5'-GATGACAAGCTTCCCATCTCG-3' were used. Relative mRNA transcript levels were obtained using an equal number of cells with simultaneous cDNA amplification within the linear range. ImageQuant software (Molecular Dynamics, Sunnyvale, CA) was used to calculate mRNA expression. The results are presented as expression index, the ratio of each gene specific expression level to the expression level from the housekeeping gene, GAPDH.

Western blotting and immunoprecipitation

Cells were lysed using a modified RIPA lysis buffer with protease inhibitors. Proteins were separated on SDS-PAGE and electro-transferred to a PVDF (Millipore, Billerica, MA), membrane blocked with 1% BSA (Sigma, St. Louis, MO), 0.05% Tween-20 (Sigma) in PBS (Mediatech), and probed with an anti-VEGFR3 antibody (sc-

637 Santa Cruz Biotechnology, Santa Cruz, CA), followed by alkaline phosphatase-conjugated secondary antibody (Vector Labs, Burlingame, CA). Protein bands were visualized using an enhanced chemifluorescence detection system according to the manufacturer's protocol (GE Healthcare, Piscataway, NJ) using a Phosphor Imager (Molecular Dynamics). Membranes were stripped and re-probed with rabbit anti-actin (A-2066, Sigma) to control for loading differences between lanes.

For immunoprecipitation experiments, cells were plated in 35 mm dishes, treated with 10 µM MAZ51, 200 ng/ml VEGF-C, or vehicle (dimethyl sulfoxide or media) for various durations. Cells were washed 2 times with cold PBS containing 0.1 mM sodium orthovanadate (Sigma). Cells were lysed using modified RIPA buffer with protease and phosphatase inhibitors. Cell suspensions were centrifuged at 16000 g for 15 minutes at 4°C. Supernatants were transferred to fresh tubes and VEGFR3 was immunoprecipitated using an anti-VEGFR3 antibody for 2 h with rotation at 4°C. Protein A/G Agarose (Santa Cruz Biotechnology) was added and the samples were rotated overnight at 4°C. Samples were centrifuged at 3000 g for 1 minute and washed using modified RIPA buffer 3 times. After the last wash, samples were suspended in SDS loading buffer, boiled and separated on SDS-PAGE.

In vitro cell viability

Briefly, 1000 or 5000 cells were plated per well of a 96-well plate and allowed to adhere overnight. MAZ51 at different concentrations in different serum conditions was added to each set of triplicate wells. Plates were incubated for 24-72 h at 37°C, 5% CO₂ and 25 µl of 5 mg/ml MTT (EMD Biosciences) was added per well. Plates were incubated at 37°C for an additional 2 h. Media was removed, 100 µl of DMSO (Fisher Scientific, St. Louis MO) was added and the plate was read using an EL × 800 microplate reader (Bio-Tek, Winooski, VA).

We plated Cl66 cells at 5 × 10⁴ cells/well in a 6-well plate and allowed the cells to adhere overnight. After washing the cells, MAZ51 was added at 10, 5 or 0 µM for 24, 48 or 72 h. The number of detached cells were counted and compared to the number of attached cells counted after removal with trypsin. Absolute

VEGFR3/Flt4 autocrine pathway in mammary tumor cells

numbers were converted into percentages using the following formula: # of cells attached or detached/(attached cells + detached cells) × 100.

F-actin staining

Cl66 cells were plated on an 8-well chamber slide and allowed to adhere overnight. Cells were treated with MAZ51 or control for 1 hour. Cells were washed and fixed with 4% paraformaldehyde for 10 minutes. Cells were washed and incubated with Texas red phalloidin (Invitrogen) for 20 minutes. Cells were washed and nuclei were counterstained with DAPI. Cells were examined using a Nikon microscope and pictures were captured using the Act-2U software (Nikon, Melville, NY).

In vivo tumor growth and metastasis

Female BALB/c mice (NCI, Bethesda, MD), 6-8 weeks of age housed under pathogen free conditions were used. Cl66 cell monolayers were trypsinized and washed with Hank's balanced salt solution (HBSS) 3 times and counted using trypan blue (Sigma) exclusion dye. Single cell suspensions of 5×10^4 cells (> 90% viability) in 100 μ l were injected into the mammary fat pad. Twice a week tumor size was measured using digital calipers (Fisher Scientific, Pittsburgh, PA). Tumor volume was calculated according to the formula: volume = $W^2 \times L/2$, where W = short diameter and L = long diameter. Mice were injected intraperitoneally with MAZ51 at 10 MPK, 5 MPK or vehicle control (dimethyl sulfoxide) on days 1-7 and 14-21 following tumor inoculation. One week later mice were euthanized and primary tumor tissue, lymph nodes, lungs, and spleens were removed. Samples were processed by formalin fixation with subsequent embedding in paraffin, cryofrozen in OCT, frozen in liquid nitrogen or processed for isolation of cells.

For experimental lung metastasis, Cl66 cells (5×10^5 cells/0.1 ml HBSS/animal) were injected intravenously. The mice were euthanized when moribund. The lungs were removed, rinsed in water, and fixed in Bouin's solution for 24 h to facilitate counting of tumor nodules. The number of surface tumor nodules was counted using a dissecting microscope. Sections of the lungs were stained with hematoxylin and eosin to confirm that the nodules were breast cancer.

Survival data were collected from mice injected intravenously. All experiments were approved by the Institutional Animal Care and Use Committee of the University of Nebraska Medical Center.

Immunohistochemical (IHC) analysis

Protein expression was analyzed in paraffin-embedded primary tumors. Briefly, 4 μ m thick sections of paraffin blocks were processed for antigen retrieval by microwave citrate buffer treatment. The slides were processed for evaluation of apoptosis using the DeadEnd Colorimetric Apoptosis kit (Promega, Madison, WI) or for proliferation using an anti-PCNA (Santa Cruz Biotechnology) antibody. PCNA immunoreactivity was detected using the ABC Elite kit (Vector Laboratories) and DAB substrate (Vector Laboratories) kit per the manufacturer's instructions. A reddish brown precipitate in the cytoplasm indicated a positive reaction. Negative controls used all reagents except the primary antibody. Intensity of staining was measured by two independent observers that examined each slide.

Statistical analysis

SPSS for Windows (SPSS Inc. Chicago, IL) was used for the independent samples *t*-test (two-tailed) to compare means. *In vivo* analysis was performed using Mann-Whitney U-test of significance. A value of $p < 0.05$ was deemed significant.

Results

VEGFC and VEGFR3 expression in murine mammary tumor cells

We have previously shown that inhibition of VEGF-C using shRNA decreases tumor growth and metastasis [7]. To expand on our earlier observations we examined the VEGF-C/VEGFR3 axis in Cl66, Cl66M2 and 4T1 murine mammary cell lines. RT-PCR analysis confirmed that all three cell lines express VEGF-C and VEGFR3 (**Figure 1A**). Cl66 cells, which have moderate metastatic potential, expressed the lowest levels of VEGF-C while 4T1 cells which are highly aggressive and metastatic expressed the highest levels of VEGF-C. All three cell lines expressed two bands for VEGFR3 with 4T1 showing the highest expression of the larger

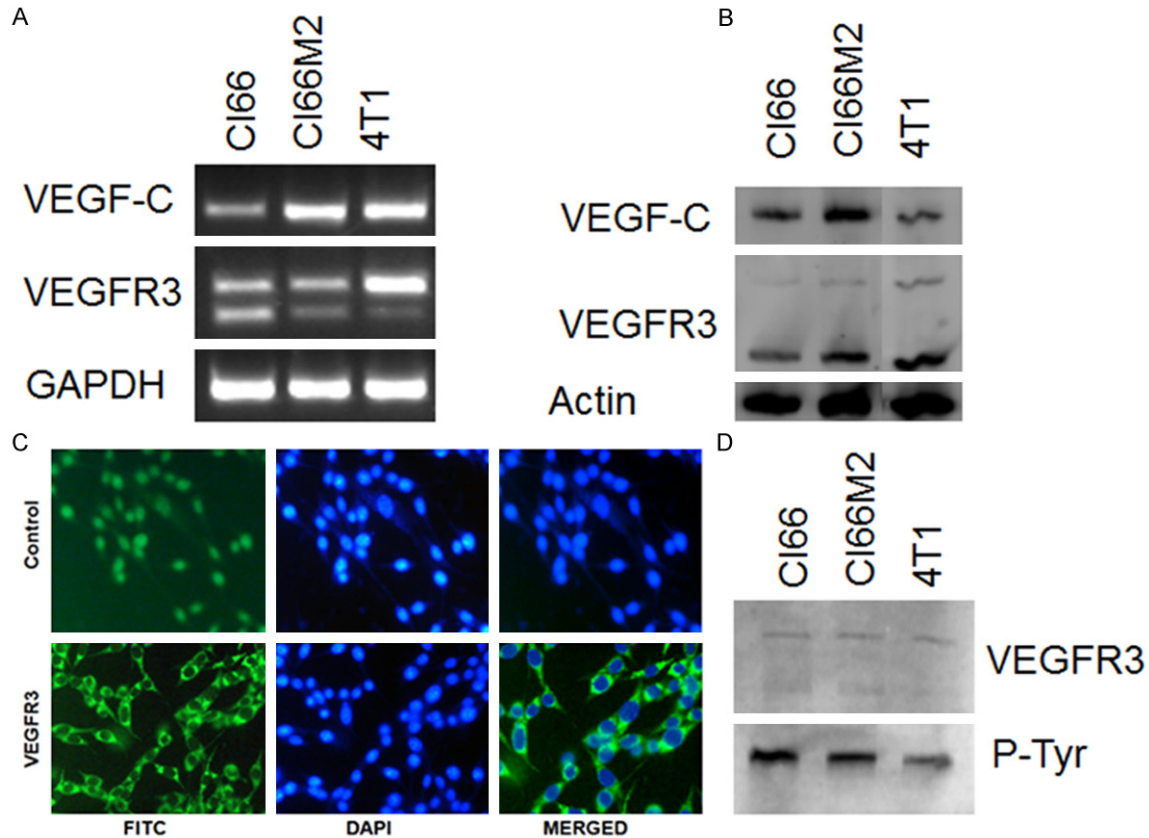


Figure 1. Expression and phosphorylation of VEGFR3 in murine mammary adenocarcinoma cells A. Expression of VEGF-C, VEGFR3, and GAPDH specific mRNA transcripts in murine mammary adenocarcinoma cell lines differing in their metastatic potential: CI66 (moderately metastatic), CI66M2 (poorly metastatic) and 4T1 (highly metastatic). B. Western blots of murine mammary adenocarcinoma cell lysates for VEGF-C, VEGFR3 and β -actin. C. Immunofluorescent staining of CI66 cells showing expression and localization of VEGFR3. D. Western blot of murine mammary adenocarcinoma cells demonstrating phosphorylation of VEGFR3 in the cells.

band and CI66 showing approximately equal expression of both sizes.

To confirm expression at the protein level we analyzed expression by Western blotting. We detected expression of VEGF-C and VEGFR3 in all cell lines (**Figure 1B**). Similarly two bands were detected for VEGFR3 by antibody detection. However, expression of the smaller molecular weight protein was more abundant with the highest level in 4T1 cells. In addition, we confirmed expression of the receptor using immunofluorescent staining (**Figure 1C**). To assess the activity of the receptor in the cells we evaluated the phosphorylation status of the receptor. Using cells which were unstimulated, we performed immunoprecipitation using an anti-VEGFR3 antibody and probed with anti-VEGFR3 and anti-p-Tyr antibodies. Results confirm expression of the receptor and its constitutive activation in all three cell lines although the

larger molecular weight protein was phosphorylated (**Figure 1D**).

VEGF-C-VEGFR3/Flt4 pathway regulates mammary tumor cell viability

These observations indicate the potential for autocrine VEGF-C/VEGFR3 signaling in this breast cancer model. To extend our previous study on the role of VEGF-C in murine mammary tumors we selected CI66 cells for our further analysis. To elucidate the role of VEGF-C, we examined the effect of inhibiting VEGF-C on viability. CI66 cells were plated and antibody to VEGFR3 (10 μ g/ml) or VEGF-C (10 μ g/ml) was added. Cells were assayed for viability at 24, 48 or 72 hours. 24 hours after addition of antibody, the viability of cells treated with VEGFR3 antibody was significantly decreased as compared to cells treated with VEGF-C antibody ($p < 0.05$) (**Figure 2A**). At 48 hours, inhibition with

VEGFR3/Flt4 autocrine pathway in mammary tumor cells

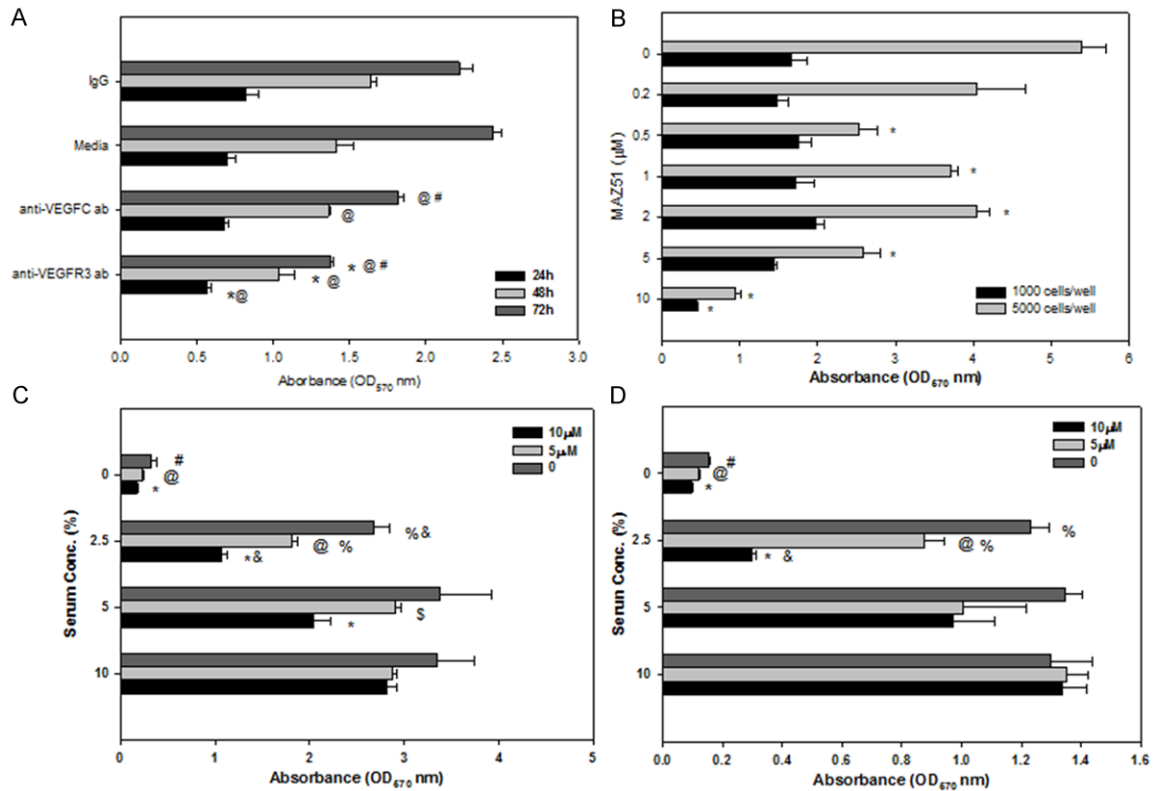


Figure 2. VEGFR3 inhibition decreases proliferation of CI66 murine mammary adenocarcinoma cells. A. 5000 CI66 cells were plated per well of a 96-well plate, treated with VEGFR3 antibody, VEGF-C antibody, IgG control or media alone and MTT absorbance was measured at 24, 48 or 72 hours after treatment $p < 0.05$ vs. *VEGF-C, vs. @IgG, vs. #media. B. 1000 or 5000 CI66 cells were plated per well of 96-well plate, treated the next day with various doses of MAZ51, and MTT absorbance was measured after 72 h. * $p < 0.05$ compared to no treatment (0 μM). C. 5000 CI66 cells were plated per well of a 96-well plate, treated the next day with 10, 5 or 0 μM MAZ51 in different serum concentrations (10, 5, 2.5 or 0%) for 72 h and MTT absorbance was measured. $p < 0.05$ vs. *10 $\mu\text{M}/10\%$, @ vs. 5 $\mu\text{M}/10\%$, # vs. 0 $\mu\text{M}/10\%$, \$ vs. 10 $\mu\text{M}/5\%$, % vs. 10 $\mu\text{M}/2.5\%$, & vs. 5 $\mu\text{M}/2.5\%$. D. 1000 CI66 cells were plated per well of a 96-well plate, treated the next day with 10, 5 or 0 μM MAZ51 in different serum concentrations (10, 5, 2.5 or 0%) for 72 h and MTT absorbance was measured. $P < 0.05$ vs. *10 $\mu\text{M}/10\%$, @ vs. 5 M/10%, # vs. 0 M/10%, % vs. 10 $\mu\text{M}/2.5\%$, & vs. 5 $\mu\text{M}/2.5\%$. The values are average + SEM.

VEGFR3 or VEGF-C antibody significantly reduced the viability of CI66 in comparison to control antibody treated cells ($p < 0.05$). By 72 hours the inhibitory effect was more dramatic.

Since we detected expression of both VEGFR3 and its ligand VEGF-C in murine mammary cancer cell lines, we wanted to expand our observations of the role of VEGFR3 as an autocrine signaling factor. Therefore, we treated CI66 cells with MAZ51, which is a cell permeable VEGFR3 tyrosine kinase inhibitor. Cells treated with MAZ51 responded in a dose-dependent manner, with a maximal inhibitory effect seen at the 10 μM dose ($p < 0.05$) (Figure 2B). At high cell density (5000 cells/well) MAZ51 significantly inhibited viability ($p < 0.05$) at all doses except for 0.2 μM . At low cell density,

viability was only inhibited significantly at 10 μM .

Next, we wanted to determine the effect of stress on the cells. To do this, we analyzed viability under decreased serum conditions. Cells were plated at 1000 or 5000 cells/well, treated with 10, 5 or 0 μM MAZ51 for 72 hours. Cells treated in media containing 10% serum were not inhibited after incubation with MAZ51 irrespective of the cell density or dose of MAZ51 (Figure 2C and 2D). There was no effect of lowering the serum to 5% on cells plated at low cell density. However, when cells were plated at a higher density of 5000 cells/well, we did observe a significant decrease in the viability of cells incubated with 10 μM MAZ51 at 5% or 2.5% serum compared to the same dose in

VEGFR3/Flt4 autocrine pathway in mammary tumor cells

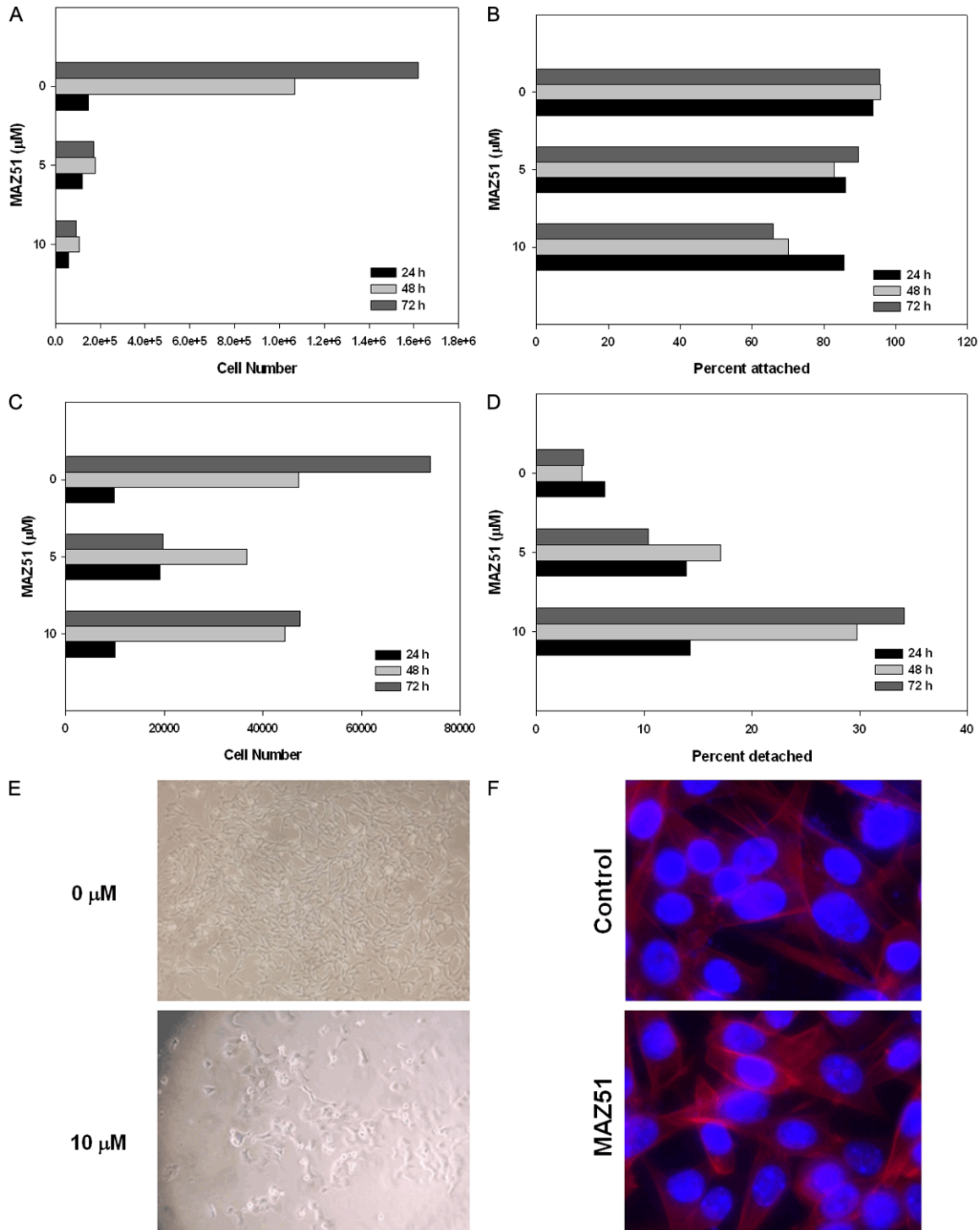


Figure 3. VEGFR3 antagonist decreases cell adhesion. 50000 CI66 cells were plated per well of a 6 well plate and the next day treated with 0, 5 or 10 μM MAZ51 for 24, 48 or 72 hours. Detached cells in the supernatant were collected and counted. Attached cells were trypsinized and counted. A. Absolute number of attached cells. B. Percentage of total attached cells. C. Absolute number of detached cells. D. Percentage of detached cells. E. Images of cells treated and counted after 24, 48 or 72 h treatment with 0, 5 or 10 μM MAZ51. F. VEGFR3 antagonist affects F-actin rearrangement. 10000 CI66 cells were plated per well of an 8-well chamber slide, treated the next day with 0 or 10 μM MAZ51 for 1 hour and stained for F-actin.

10% serum ($p < 0.05$). However, we did not observe changes in viability at 5 μM MAZ51

unless cells were incubated in less than 5% serum. In 2.5% serum-containing media, cells

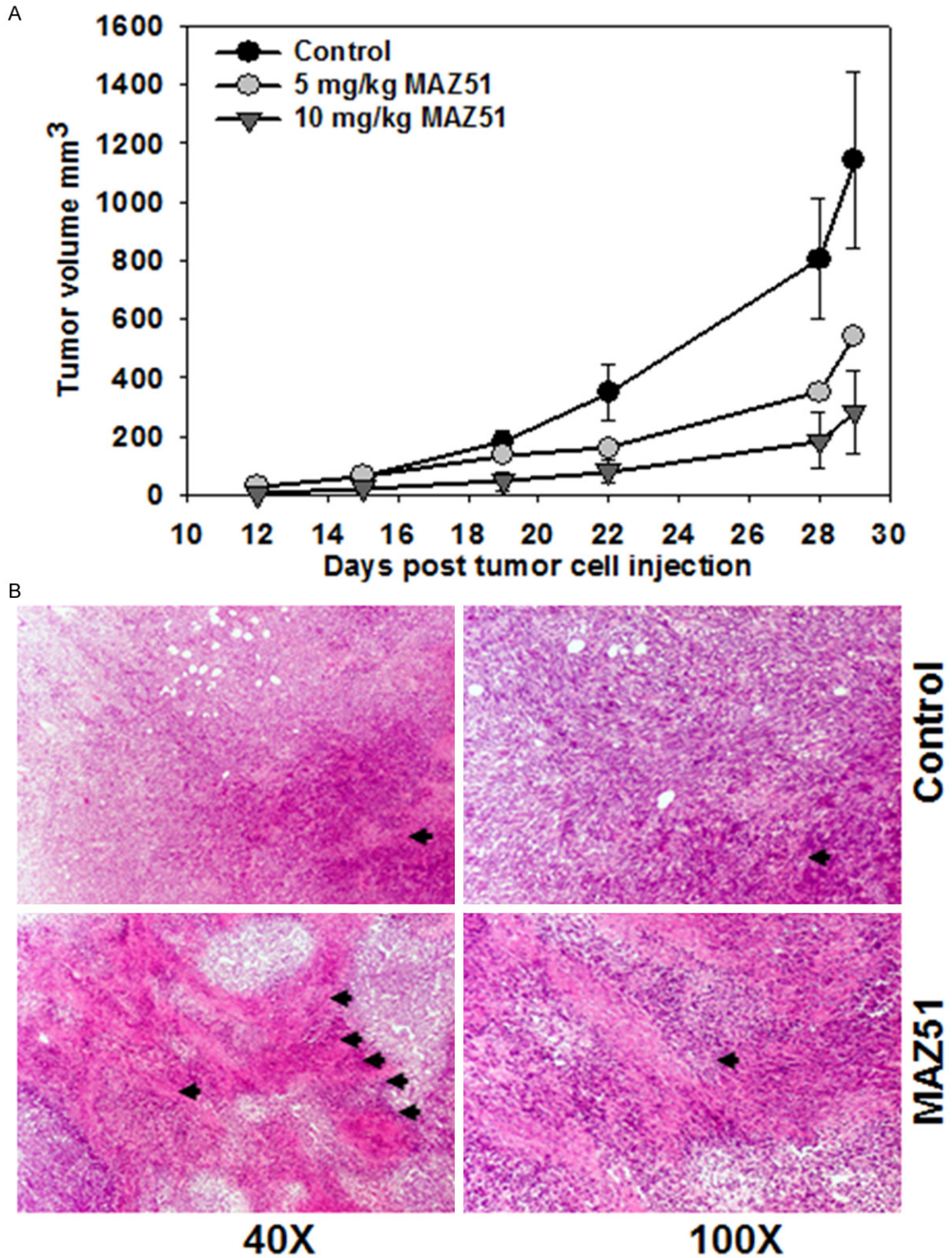


Figure 4. VEGFR3 antagonist inhibits tumor growth. A. *In vivo* tumor growth curve of Cl66 tumor-bearing mice treated with control (DMSO), 5, or 10 mg/kg MAZ51. B. Representative H&E sections from tumors of control tumor-bearing mice or 10 mg/kg-treated mice. Arrows indicate tumor cells.

plated at a low cell density showed a decrease in viability after treatment with either 10 or 5

μM MAZ51 as compared to no MAZ51 treatment ($p < 0.05$).

VEGFR3/Flt4 autocrine pathway in mammary tumor cells

As a result of these experiments we wanted to determine if the effect on viability was a result of increased cell death or an inhibition of cellular proliferation. Control treated cells exhibited an increase in the absolute number of cells which attached at 72 h, while we did not detect changes in the absolute number of cells attached after treatment with MAZ51 at any of the time points (**Figure 3A**). The overall number of detached cells did not differ among groups until 72 h when the cells treated with MAZ51 showed less detached cells as compared to control cells (**Figure 3B**). Since there was an increase in the absolute number of cells attached in the control group we compared the percent cells attached and detached to determine the overall effect of the inhibitor on the cells. When the numbers were converted to percent cells attached there was no difference in attachment (**Figure 3C**), however there was a marked increase in detachment of cells after treatment with MAZ51 (**Figure 3D**). Observation of the cells after treatment with MAZ51 revealed an interesting change in the morphology of the cells. The appearance of the cells indicated that there was a difference in the behavior of the cells as the cells were no longer forming focal adhesions and tight networks of cells (**Figure 3E**).

Based on these results, we treated the cells with MAZ51 and looked for apoptosis using TUNEL staining. We did not observe an increase in apoptosis (data not shown) after treatment.

Since we detected morphological changes in the cells, we stained the cells after treatment with MAZ51 to look for changes in cytoskeletal arrangement. As shown in **Figure 3F**, treatment with MAZ51 caused F-actin fiber re-arrangement.

VEGFR3 antagonist inhibits mammary tumor growth and metastasis

Based on our *in vitro* studies and a previous report from our group showing inhibition of tumor growth and metastases in mice after knocking-down VEGF-C, we injected Cl66 murine mammary cancer cells into mice. Following inoculation of tumor cells into the mammary fat pad, mice were treated with different doses of MAZ51 or vehicle control as described in materials and methods. Tumor growth was inhibited in mice treated with either

5 or 10 MPK as compared to vehicle alone (**Figure 4A** and **4B**). We did not observe any difference in animal weight suggesting MAZ51 was well-tolerated (data not shown). Lymph nodes were measured and we detected a decrease in lymph node size for mice injected with the 10 MPK dose of MAZ51 (data not shown). We did not detect any differences in the WBC counts of spleens or the number of tumor-associated lymphocytes among the groups (data not shown).

Mice treated with MAZ51 had a lower overall incidence of spontaneous lung metastases, with a lower median number of nodules which were smaller in size (**Figure 5A** and **5B**). However, when mice were injected with Cl66 cells intravenously and treated with MAZ51, there was no detectable difference in the median number of lung nodules.

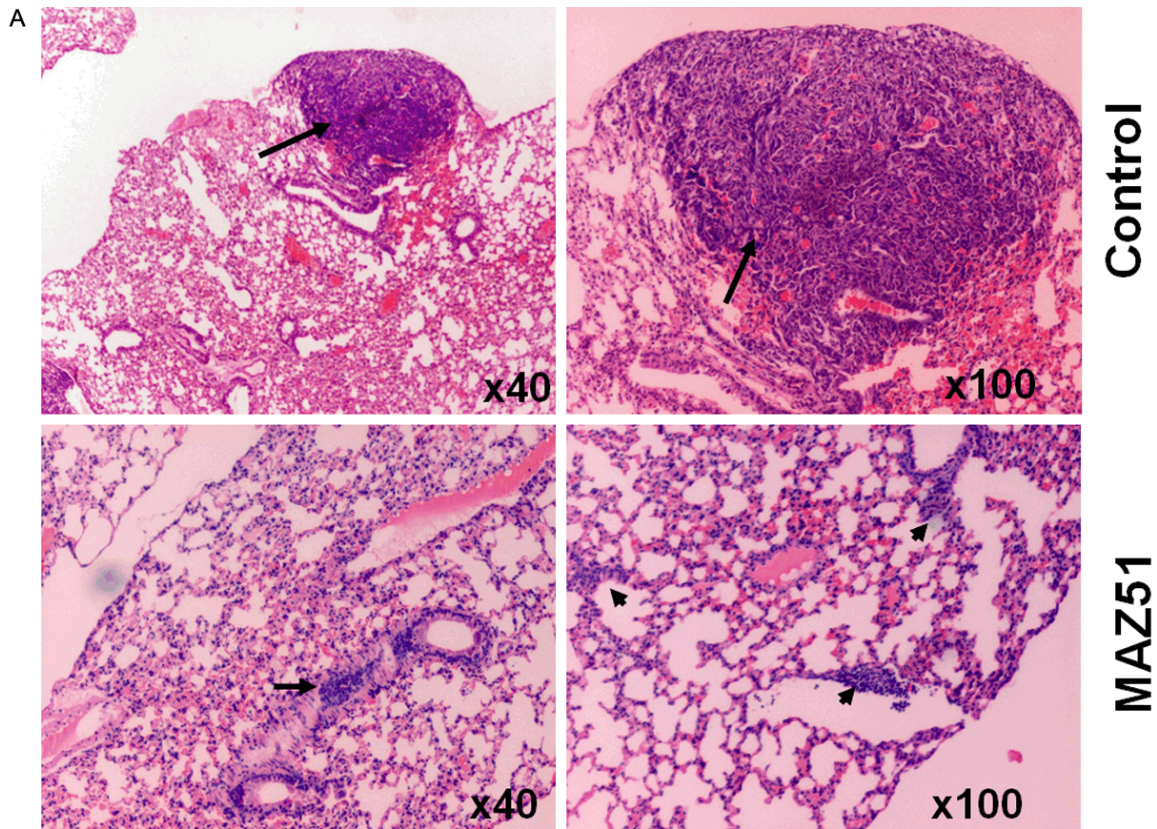
Interestingly, expression of VEGFR3 mRNA in tumors of mice treated with MAZ51 was increased as compared to control mice at the mRNA level (**Figure 5C**). ELISA for secreted VEGF-C did not show any detectable difference among the groups from either tumors or serum (data not shown). In addition, we performed RT-PCR for other VEGF receptors and molecules and did not detect any differences in the expression of other VEGF family members, including VEGFR1, VEGFR2, VEGF-A, VEGF-B and VEGF-D (data not shown).

Decreased in situ tumor cell proliferation and survival in mammary tumors following treatment with VEGFR3 antagonist

To elucidate the mechanism of the decrease in *in vivo* tumor growth and metastasis, tumor samples were evaluated immunohistochemically for proliferation and apoptosis markers. Tumor sections were stained for PCNA and TUNEL. Evaluation of PCNA staining revealed that MAZ51-treated tumors had slightly lower numbers of proliferating cells although not statistically significant (**Figure 6A**). TUNEL stained sections of MAZ51-treated tumors had a significantly higher overall score compared to control-treated tumors (**Figure 6B**).

Discussion

In this study we wanted to expand our previous observations that down-regulation of VEGF-C in breast cancer cells decreased tumor growth



B

Spontaneous lung metastasis		
	Incidence	Median (range)
Control	100%	8 (3-11)
MAZ51 10	30%	2 (0-5)

C

Experimental lung metastasis		
	Incidence	Median (range)
Control	100%	50 (25-65)
MAZ51 10	100%	52 (23-77)

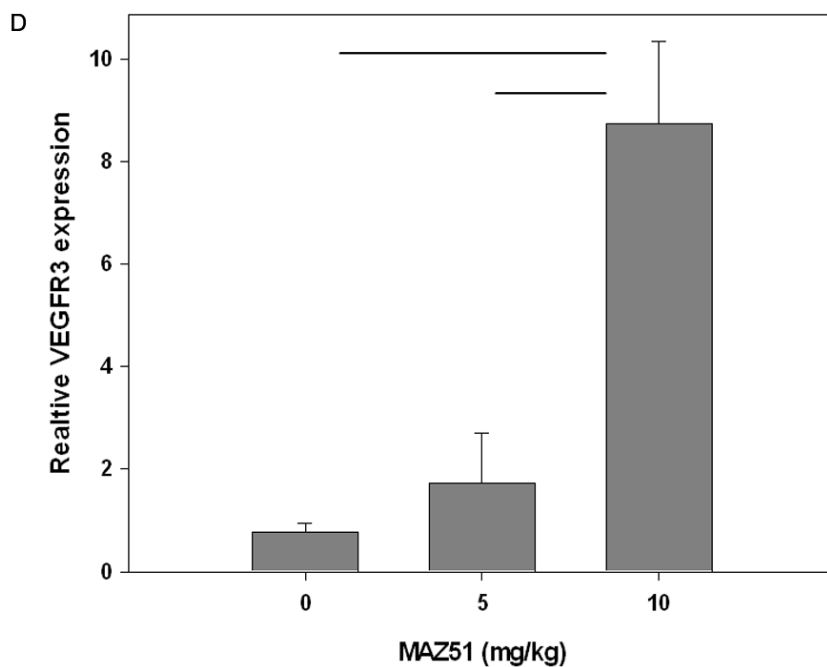
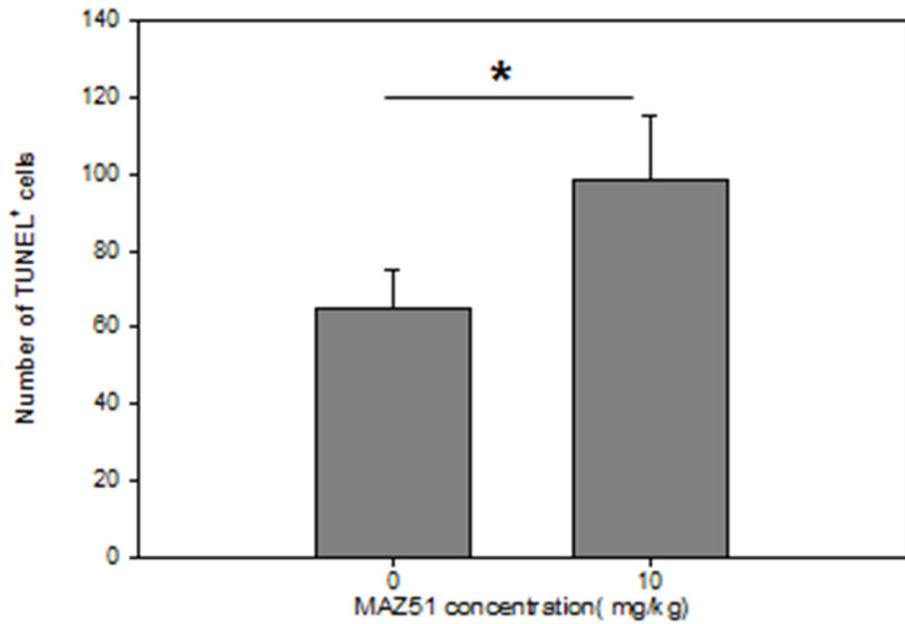
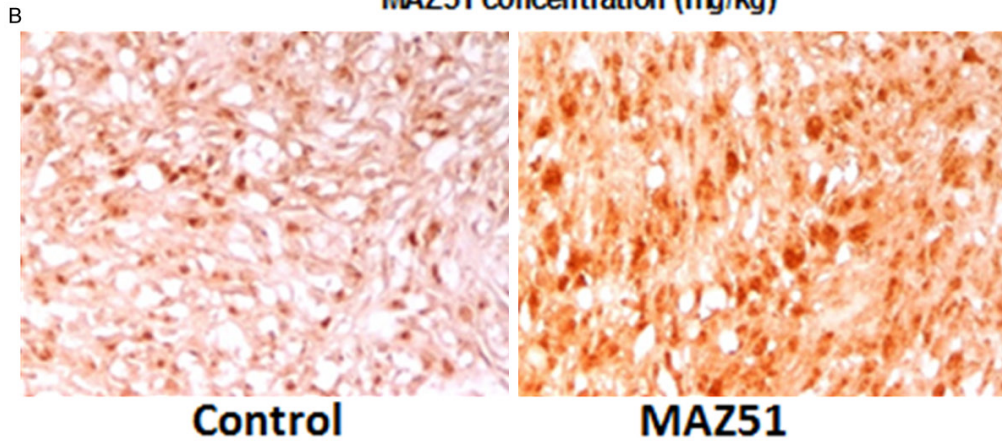
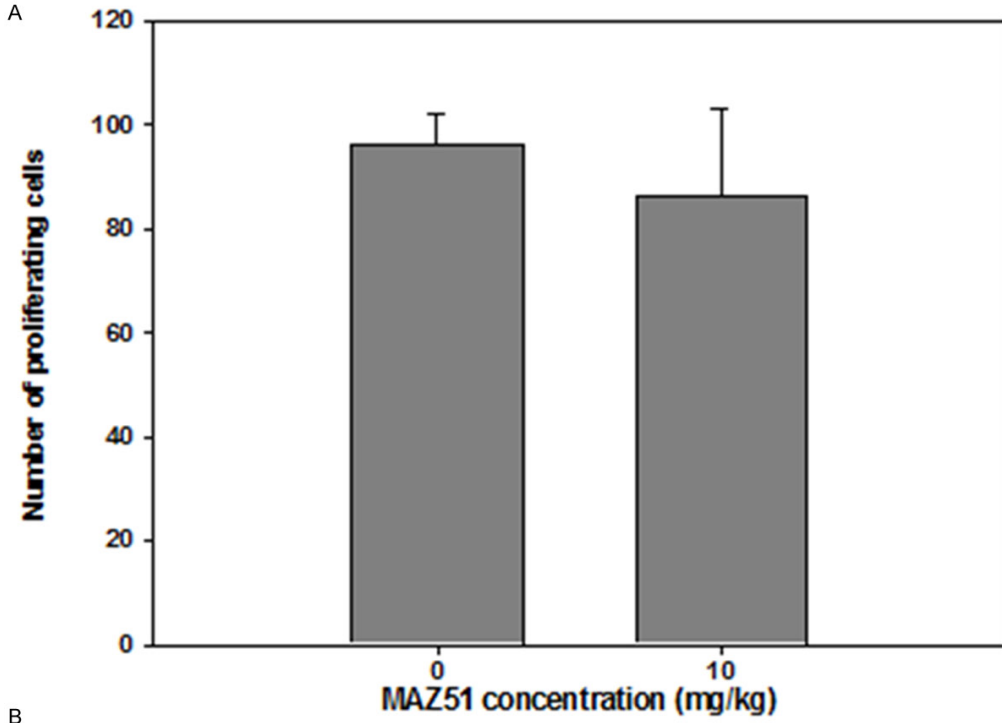


Figure 5. VEGFR3 antagonist inhibits tumor metastasis. A. Representative H&E sections from lungs of control tumor-bearing mice or 10 mg/kg-treated mice. Arrows indicate micrometastatic nodules in lungs. B. Incidence and median of metastatic lung nodules in mammary fat pad tumor-bearing mice. C. Incidence and median of metastatic lung nodules in IV-injected mice. D. Relative mRNA expression in tumors from mice treated with 0, 5, or 10 mg/kg MAZ51. * $p < 0.05$ vs. 10.

VEGFR3/Flt4 autocrine pathway in mammary tumor cells



VEGFR3/Flt4 autocrine pathway in mammary tumor cells

Figure 6. VEGFR3 antagonist enhanced *in situ* tumor cell apoptosis. A. Quantitation of PCNA⁺ cells in tumors from mice treated with 0 or 10 mg/kg MAZ51. B. Quantitation of TUNEL⁺ cells in tumors from mice treated with 0 (control) or 10 mg/kg MAZ51. *p < 0.05 vs. 0.

and metastasis. In order to accomplish this, we focused on understanding the interaction of VEGF-C with its receptor, VEGFR3 in breast cancer cells. We found that not only do breast cancer cells express VEGFR3, but the receptor is active by the evidence of constitutive phosphorylation. In addition, blocking the VEGF-C/VEGFR3 pathway interfered with the ability of breast cancer cells to proliferate. Preventing the interaction of VEGF-C with VEGFR3 *in vivo* resulted in decreased tumor and metastatic burden.

Several studies have shown the expression of VEGF-C and VEGFR3 in different tumor types [9-11]. Similarly we detected expression of both VEGF-C and VEGFR3 in murine breast cancer cells and the receptor was constitutively activated. To extend these observations to better understand the importance of this axis in the autocrine regulation of CI66 cells, we treated cells with an anti-VEGFR3 antibody. As soon as 24 hours after cells were treated with an anti-VEGFR3 antibody an inhibitory effect was seen and that trend continued for the duration of the treatment.

MAZ51 is a cell permeable tyrosine kinase inhibitor, which has been shown to inhibit the phosphorylation of VEGFR3 [8]. To elucidate more specifically about the function of the receptor in this system we treated cells with MAZ51. Cells treated with MAZ51 in normal serum containing medium were not significantly inhibited. However when the serum concentration was reduced cell viability was significantly decreased in conjunction with treatment. Reduced serum concentrations simulate *in vivo* stress conditions, thus indicating the potential importance of this signaling axis *in vivo*.

To better understand the changes in viability we detected by MTT, we counted absolute numbers of cells. Our results indicated the cells undergoing treatment with the inhibitor were detaching from the plate. Additionally, observation of the cells *in vitro* during treatment with MAZ51 revealed alterations in the cells. We did not detect an increase in apoptosis of the cells undergoing treatment, but further investigation into this mechanism is warranted to under-

stand what is modulating the viability of the cells. We speculate since it is essential for metastatic cells to avoid undergoing anoikis, to be able to survive when they are separated from the primary tumor [12] it is possible VEGFR3 may play a role in this system in protecting cells from anoikis. A recent paper by Stanton et al showed the importance of the VEGF-C/NRP-2 axis in autophagy control [13]. Therefore it is possible that under stressful conditions VEGFR3 may play a role in inducing autophagy and inhibiting this may cause the cells to die. Based on our observations it would appear that VEGFR3 plays an important role in aiding cellular viability and blocking VEGFR3 signaling hinders this ability. This may also provide an explanation for the decreased metastasis that we observed *in vivo*. This is supported by a study by Feng et al suggesting that VEGF-C siRNA mediated knockdown in lung cancer cells decreases invasion and arrests the tumor cells in the G1 phase suggesting the requirement for VEGF-C in the metastatic cascade [14].

A report from Wang et. al. suggests that VEGFR3 protects against oxidative stress in endothelial cells [15]. Similarly, we found under conditions of increased stress (low serum concentration) that inhibiting VEGFR3 signaling resulted in lower cellular viability. Alongside these observations Garces et. al. using phage display found that VEGFR3 bound to focal adhesion kinase (FAK), which suppressed apoptosis and interference with this binding decreased proliferation and caused apoptosis in human breast cancer cells [16]. The morphological changes we observed in cells undergoing treatment with MAZ51 showed that cells appeared to be making fewer focal adhesion contacts suggesting lower expression of FAK. This is a potential explanation for the decrease in cellular viability we observed. Further studies will be needed to confirm these interpretations.

Mice treated with soluble antibody to VEGFR3 that blocks receptor signaling have decreased tumor growth, lymphangiogenesis and metastasis [17]. In line with these results, when mice were inoculated with CI66 murine breast cancer cells and treated with MAZ51, tumor growth and metastasis were decreased. Similar to our

in vitro results, we saw an increase in areas of necrosis in the treated tumors as compared to untreated tumors. When mice were injected intravenously, we did not see a decrease in lung lesions, reinforcing the importance of inhibiting the VEGFR3 pathway in the initiation of metastasis.

Taken together our results along with the results of others suggest strongly the potential for exploiting the VEGF-C/VEGFR3 signaling axis as a therapeutic target in breast cancer.

Acknowledgements

This work was supported in part by Susan G. Komen for the Cure grant KG090860 COBRE grant RR021937 (Nebraska Center for Nanomedicine), and Cancer Center Support Grant (P30CA036727) from National Cancer Institute, and National Institutes of Health.

Disclosure of conflict of interest

Authors declare no conflict of interest.

Abbreviations

VEGF-C, Vascular endothelial growth factor-C; VEGFR3, Vascular Endothelial growth Factor Receptor-3; MPK, mg/kg.

Address correspondence to: Rakesh K Singh, Department of Pathology and Microbiology, The University Nebraska Medical Center, 985900 Nebraska Medical Center, Omaha NE 68198-5900. Tel: 402-559-9949; Fax: 402-559-5900; E-mail: RSINGH@UNMC.EDU

References

- [1] Siegel R, Ma J, Zou Z, Jemal A. Cancer statistics, 2014. *CA Cancer J Clin* 2014; 64: 9-29.
- [2] Weigelt B, Peterse JL, van 't Veer LJ. Breast cancer metastasis: markers and models. *Nat Rev Cancer* 2005; 5: 591-602.
- [3] Mohammed RA, Green A, El-Shikh S, Paish EC, Ellis IO, Martin SG. Prognostic significance of vascular endothelial cell growth factors -A, -C and -D in breast cancer and their relationship with angio- and lymphangiogenesis. *Br J Cancer* 2007; 96: 1092-100.
- [4] Su JL, Yang PC, Shih JY, Yang CY, Wei LH, Hsieh CY, Chou CH, Jeng YM, Wang MY, Chang KJ, Hung MC, Kuo ML. The VEGF-C/Flt-4 axis promotes invasion and metastasis of cancer cells. *Cancer Cell* 2006; 9: 209-23.
- [5] Kurenova EV, Hunt DL, He D, Fu AD, Massoll NA, Golubovskaya VM, Garces CA, Cance WG. Vascular endothelial growth factor receptor-3 promotes breast cancer cell proliferation, motility and survival in vitro and tumor formation in vivo. *Cell Cycle* 2009; 8: 2266-80.
- [6] Laakkonen P, Waltari M, Holopainen T, Takahashi T, Pytowski B, Steiner P, Hicklin D, Persaud K, Tonra JR, Witte L, Alitalo K. Vascular endothelial growth factor receptor 3 is involved in tumor angiogenesis and growth. *Cancer Res* 2007; 67: 593-9.
- [7] Chen Z, Varney ML, Backora MW, Cowan K, Solheim JC, Talmadge JE, Singh RK. Down-regulation of vascular endothelial cell growth factor-C expression using small interfering RNA vectors in mammary tumors inhibits tumor lymphangiogenesis and spontaneous metastasis and enhances survival. *Cancer Res* 2005; 65: 9004-11.
- [8] Kirkin V, Thiele W, Baumann P, Mazitschek R, Rohde K, Fellbrich G, Weich H, Waltenberger J, Giannis A, Sleeman JP. MAZ51, an indolinone that inhibits endothelial cell and tumor cell growth in vitro, suppresses tumor growth in vivo. *Int J Cancer* 2004; 112: 986-93.
- [9] Jennbacken K, Vallbo C, Wang W, Damber JE. Expression of vascular endothelial growth factor C (VEGF-C) and VEGF receptor-3 in human prostate cancer is associated with regional lymph node metastasis. *Prostate* 2005; 65: 110-6.
- [10] Jenny B, Harrison JA, Baetens D, Tille JC, Burkhardt K, Mottaz H, Kiss JZ, Dietrich PY, De Tribolet N, Pizzolato GP, Pepper MS. Expression and localization of VEGF-C and VEGFR-3 in glioblastomas and haemangioblastomas. *J Pathol* 2006; 209: 34-43.
- [11] Zhang J, Ji J, Yuan F, Zhu L, Yan C, Yu YY, Liu BY, Zhu ZG, Lin YZ. Cyclooxygenase-2 expression is associated with VEGF-C and lymph node metastases in gastric cancer patients. *Biomed Pharmacother* 2005; 59 Suppl 2: S285-S288.
- [12] Geiger TR, Peeper DS. Metastasis mechanisms. *Biochim Biophys Acta* 2009; 1796: 293-308.
- [13] Stanton MJ, Dutta S, Zhang H, Polavaram NS, Leontovich AA, Hönscheid P, Sinicrope FA, Tindall DJ, Muders MH, Datta K. Autophagy control by the VEGF-C/NRP-2 axis in cancer and its implication for treatment resistance. *Cancer Res* 2013; 73: 160-71.
- [14] Feng Y, Hu J, Ma J, Feng K, Zhang X, Yang S, Wang W, Zhang J, Zhang Y. RNAi-mediated silencing of VEGF-C inhibits non-small cell lung cancer progression by simultaneously down-regulating the CXCR4, CCR7, VEGFR-2 and VEGFR-3-dependent axes-induced ERK, p38 and AKT signalling pathways. *Eur J Cancer* 2011; 47: 2353-63.

VEGFR3/Flt4 autocrine pathway in mammary tumor cells

- [15] Wang JF, Zhang X, Groopman JE. Activation of vascular endothelial growth factor receptor-3 and its downstream signaling promote cell survival under oxidative stress. *J Biol Chem* 2004; 279: 27088-97.
- [16] Garces CA, Kurenova EV, Golubovskaya VM, Cance WG. Vascular endothelial growth factor receptor-3 and focal adhesion kinase bind and suppress apoptosis in breast cancer cells. *Cancer Res* 2006; 66: 1446-54.
- [17] Lin J, Lalani AS, Harding TC, Gonzalez M, Wu WW, Luan B, Tu GH, Koprivnikar K, VanRoey MJ, He Y, Alitalo K, Jooss K. Inhibition of lymphogenous metastasis using adeno-associated virus-mediated gene transfer of a soluble VEGFR-3 decoy receptor. *Cancer Res* 2005; 65: 6901-9.